

Cancer-derived exosomes loaded with ultrathin Palladium nanosheets for targeted bioorthogonal catalysis

María Sancho-Albero^{1,2,#} *Belén Rubio-Ruiz*^{3,±,#} *Ana M. Pérez-López*^{3,#} *Víctor Sebastián*^{1,2,#} *Pilar Martín-Duque*⁴ *Manuel Arruebo*^{1,2} *Jesús Santamaría*^{1,2,*} and *Asier Unciti-Broceta*^{3,*}

¹ Department of Chemical Engineering, Aragon Institute of Nanoscience, University of Zaragoza, Campus Río Ebro-Edificio I+D, c/Poeta Mariano Esquillor s/n, 50018 Zaragoza, Spain

² Networking Research Center on Bioengineering, Biomaterials and Nanomedicine (CIBER-BBN), 28029 Madrid, Spain

³ Cancer Research UK Edinburgh Centre, MRC Institute of Genetics & Molecular Medicine, University of Edinburgh, Crewe Road South, Edinburgh EH4 2XR, UK

⁴ Instituto Aragonés de Ciencias de la Salud// Fundación Araid// IIS Aragón. Centro de Investigaciones Biomédicas de Aragón, Avda San Juan Bosco 13, 50009 Zaragoza, Spain

*Email: jesus.santamaría@unizar.es; Asier.Unciti-Broceta@igmm.ed.ac.uk

Table of contents

1. SUPPLEMENTARY METHODS	2
1.1. General	
1.2. Preparation of materials	2
1.2.1. Exosome purification	2
1.2.2. Synthesis of Palladium-labile on-off sensor 1	3
1.2.3. Synthesis of prodrug 4	5
1.3. Physical and functional characterization	8
1.3.1. Electron microscopy: TEM imaging	8
1.3.2. UV-VIS Spectroscopy	8
1.3.3. Inductively coupled plasma mass spectrometry (ICP-MS)	9
1.3.4. Energy-dispersive X-ray spectroscopy analysis	10
1.3.5. X-Ray Photoelectron Spectroscopy	11
1.3.6. Native Western blot	11
1.3.7. Stability study	12
1.3.8. Fluorescence spectra of compounds 1 and 2	13
1.3.9. Time lapse imaging	13
1.3.10. Determination of the reaction rate constant (<i>K</i>)	14
1.3.11. Recyclability study of Pd-Exo ^{A549}	15
1.4. Biological experiments	15
1.4.1. Study of Pd-Exo ^{A549} biocompatibility	15
1.4.2. Confocal study of Pd-Exo ^{A549} cell internalization	16
1.4.3. Cell viability study in A549 and U87 cells: 4 vs 3	19
1.4.4. Synergistic cytotoxic study between 3 and Pd-Exo ^{A549} in A549 cells	19
1.4.5. Exo ^{A549} -mediated uncaging of 4 in A549 cells	20
1.4.6. Pd-Exo ^{A549} -mediated activation of 4 at a range of concentrations	20
1.4.7. Catalytic properties of Pd-Exo ^{A549} versus Pd-Exo ^{U87}	21
1.4.8. Cell viability and intracellular prodrug activation study in RAW cells	22
1.4.9. Target engagement assay	23
2. SUPPLEMENTARY REFERENCES	24

1. SUPPLEMENTARY METHODS

1.1. General

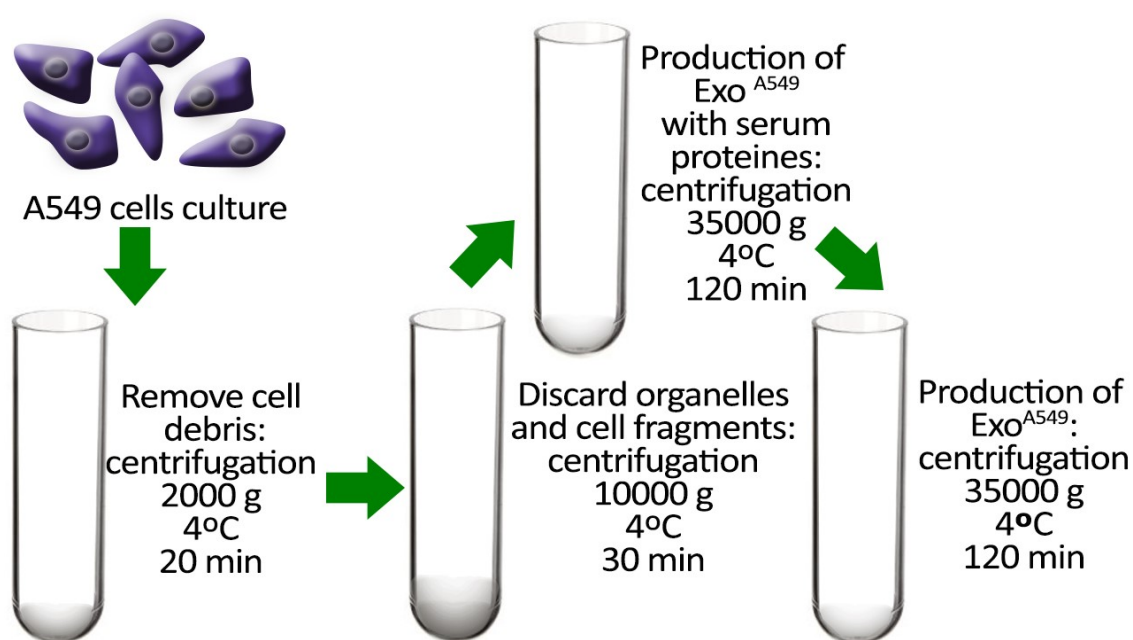
Chemicals and solvents were purchased from Fisher Scientific, Sigma-Aldrich, VWR International Ltd or TCI UK Ltd. Panobinostat (**3**) was purchased from LC Laboratories. NMR spectra were recorded at ambient temperature on a 500 MHz Bruker Avance III spectrometer. Chemical shifts are reported in parts per million (ppm) relative to the solvent peak. R_f values were determined on Merck TLC Silica gel 60 F254 plates under a 254 nm UV source. Purifications were carried out by flash column chromatography using commercially available silica gel (220-440 mesh, Sigma-Aldrich) or via semipreparative TLC chromatography on Merck TLC Silica gel 60 F254 plates. High Resolution Mass Spectrometry was measured in a Bruker MicrOTOF II. Compounds purity was >95% as measured by either TLC and NMR or HPLC using an Agilent 1200 system. Method: eluent A: water and formic acid (0.1 %); eluent B: acetonitrile and formic acid (0.1 %); A/B = 95:5 isocratic 0.5 min, 95:5 to 0:100 in 4.5 min, isocratic 2 min, 0:100 to 95:5 in 0.5 min, and isocratic 2.5 min (flow = 0.2 mL / min). Stock solutions (100 mM) were prepared in DMSO. Antibodies employed for Western Blot analysis were purchased from Abcam, Santa Cruz Biotechnology, BD Bioscience and Cell Signaling Technologies.

1.2. Preparation of materials

1.2.1. Exosome purification

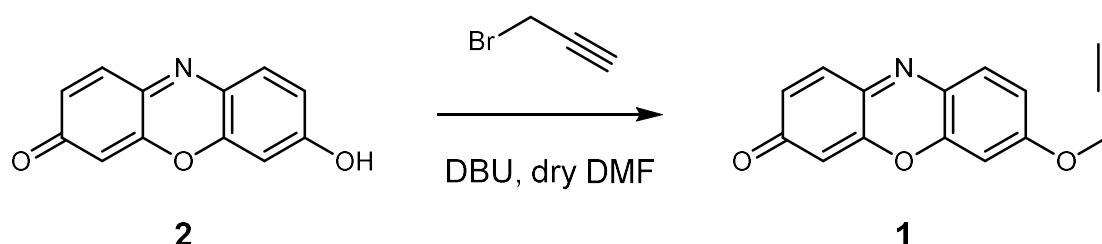
A549 cells were cultured in Dulbecco's modified Eagle's medium (DMEM) supplemented with 10 % foetal bovine serum (FBS), 1 % penicillin/streptomycin and 1 % amphotericin, under normoxic conditions. Ultracentrifuged serum (Ultracene medium, 100,000 g, 8 h, 4 °C) was employed to guarantee exosomes free medium. **Exo**^{A549} were collected and purified by successive ultracentrifugation cycles from supernatants of A549 cell culture at confluency. The first cycle was carried out at 2,000 g and 4 °C for 20 min. A second ultracentrifugation step was then carried out at 10,000 g and 4 °C for 30 min to sediment and discard organelles, cell fragments and microvesicles. To isolate the exosome fraction, the samples were ultracentrifuged at 35,000 g and 4 °C for 2 h twice (in order to eliminate the proteins superficially bound to exosomes). Isolated **Exo**^{A549} were resuspended in PBS and characterized by a Pierce BCA protein assay (Thermo Fisher Scientific) to estimate protein content. The total amount of protein present in the exosomes samples was quantified by measuring the absorption spectra and comparing it with BSA solutions of known concentration provided.

Same procedure but using U87 cells was used to purified **Exo**^{U87}.

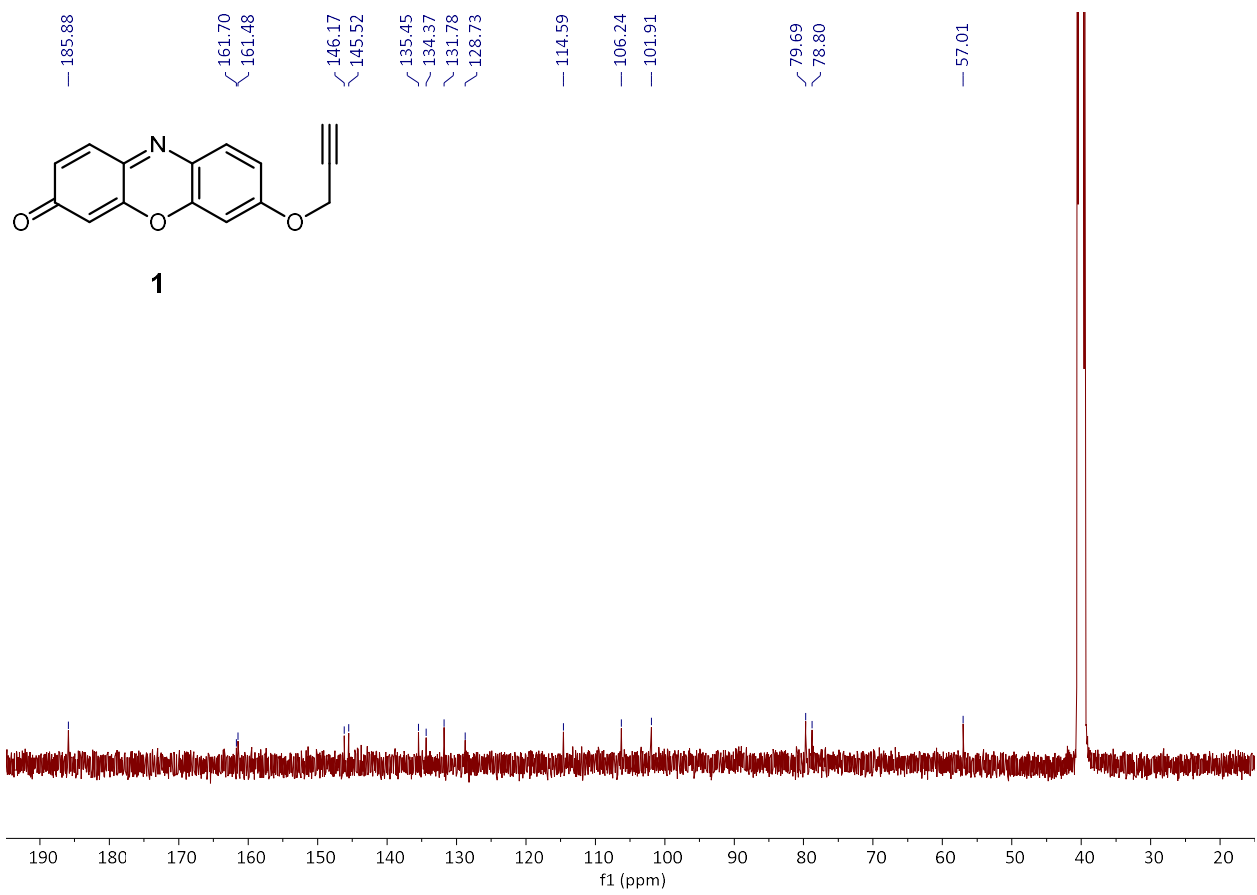
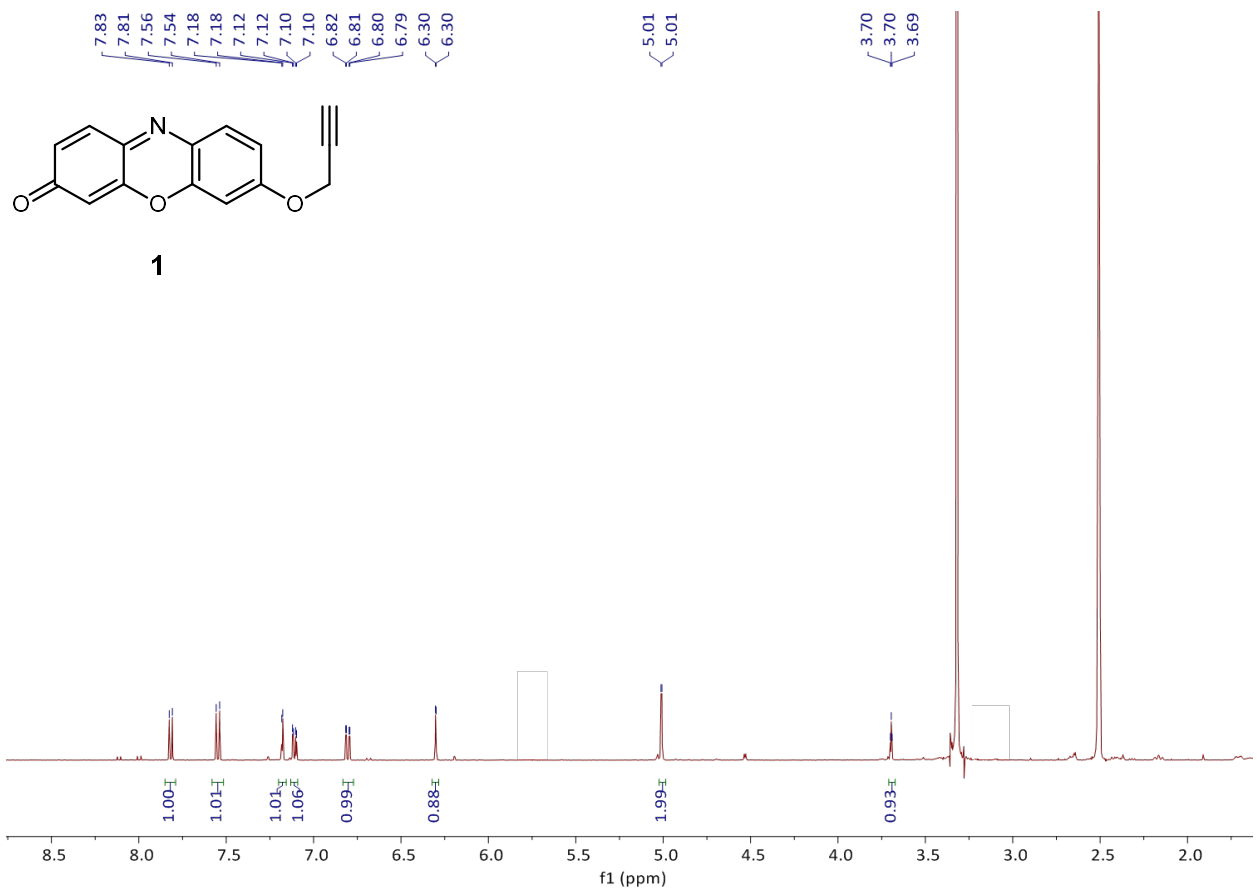


Suppl. Fig. 1. Purification protocol of exosomes derived from A549 cells.

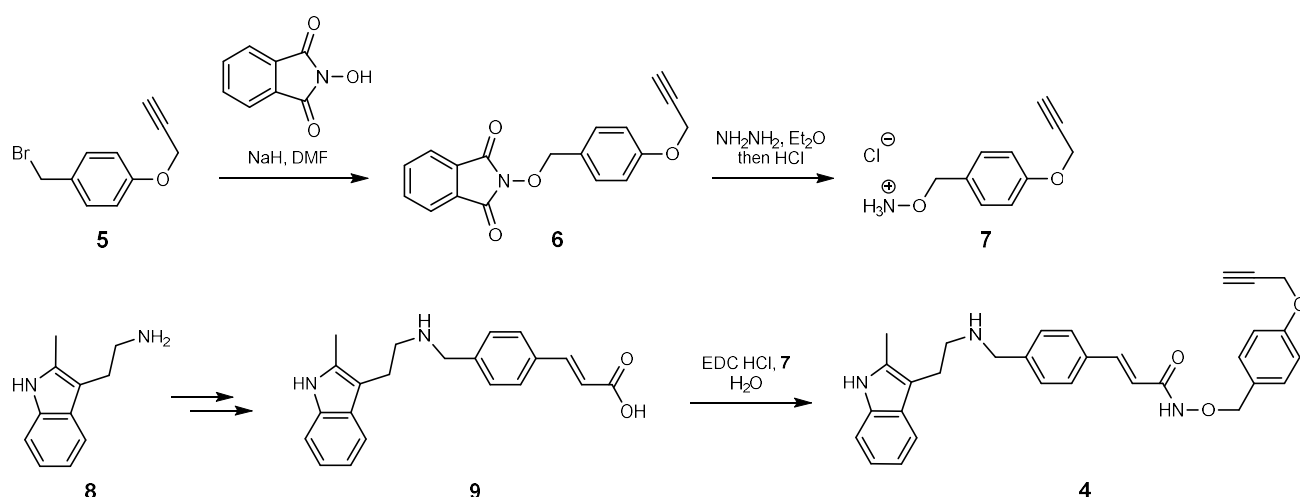
1.2.2. Synthesis of Palladium-labile on-off sensor 1



Resorufin **2** (300 mg, 1.4 mmol) and DBU (390 μ L, 2.8 mmol) was dissolved in dry DMF (5 mL) under N₂ atmosphere. Propargyl bromide (240 μ L, 2.8 mmol) was dissolved in dry DMF (0.5 mL) and was added dropwise to the previous solution. The resulting mixture was stirred at rt for 18 h. Solvent was then removed under reduced pressure, and DCM was added to get a solid precipitated. The mixture was filtered off and the filtrate was washed with H₂O (2 x 10 mL) in a separating funnel. The organic layer was dried using anhydrous MgSO₄ and the crude purified via semipreparative TLC chromatography (2.5% MeOH in CH₂Cl₂) to yield **1** (7-Propargyloxy-3H-phenoxazin-3-one) as an orange solid (75 mg, 21% yield). R_f = 0.35 (5% MeOH in CH₂Cl₂). **¹H NMR** (500 MHz, DMSO-d₆) δ 7.82 (d, *J* = 8.9 Hz, 1H), 7.55 (d, *J* = 9.8 Hz, 1H), 7.18 (d, *J* = 2.7 Hz, 1H), 7.11 (dd, *J* = 8.9, 2.7 Hz, 1H), 6.80 (dd, *J* = 9.8, 2.1 Hz, 1H), 6.30 (d, *J* = 2.0 Hz, 1H), 5.01 (d, *J* = 2.4 Hz, 2H), 3.70 (t, *J* = 2.4 Hz, 1H). **¹³C NMR** (126 MHz, DMSO-d₆) δ 185.88, 161.70, 161.48, 146.17, 145.52, 135.45, 134.37, 131.78, 128.73, 114.59, 106.24, 101.91, 79.69, 78.80, 57.01. **HRMS** (m/z): [M]⁺ calcd. for C₁₅H₁₀N₃O₁, 252.06552; found, 252.06550.



1.2.3. Synthesis of prodrug 4



Synthesis of *p*-(propargyloxy)benzyl bromide (5). 4-hydroxybenzyl alcohol was treated with propargyl bromide and K₂CO₃ to give rise *p*-(propargyloxy)benzyl alcohol, which was then converted in the corresponding halogenated intermediate using CBr₄/PPh₃.¹

Synthesis of *N*-[4-(propargyloxy)benzyloxy]phthalimide (6). Compound 6 was synthesized following the procedure previously described for other *N*-(alkyl)phthalimides.² In brief, *N*-hydroxyphthalimide (360 mg, 2.2 mmol) was dissolved in dry DMF under a nitrogen atmosphere. This solution was then added to a suspension of NaH (2.6 mmol) in DMF, yielding a red opaque solution. Then, compound 5 (4.4 mmol) in DMF was added dropwise and the reaction mixture was heated to approximately 70°C and stirred for 24 h. DMF solvent was removed at reduced pressure, the residue dissolved in CHCl₃ and washed with H₂O, NaHSO₃/ Na₂CO₃ (aq). The CHCl₃ layer was dried over anhydrous Na₂SO₄ and evaporated to dryness under reduced pressure. The resulting solid was recrystallized from hot ethanol giving rise a pale-yellow solid (534 mg, 79 % yield). **¹H NMR** (500 MHz, DMSO) δ 7.86 (s, 4H), 7.45 (d, *J* = 8.7 Hz, 2H), 7.00 (d, *J* = 8.7 Hz, 2H), 5.10 (s, 2H), 4.81 (d, *J* = 2.4 Hz, 2H), 3.56 (t, *J* = 2.4 Hz, 1H). **¹³C NMR** (126 MHz, DMSO) δ 163.12, 157.78, 134.77 (CH x 2), 131.35 (CH x 2), 128.51 (C x 2), 126.92, 123.22 (CH x 2), 114.70 (CH x 2), 79.06, 78.78 (CH₂), 78.29 (CH), 55.41 (CH₂). **HRMS** (*m/z*): [M]⁺ calcd. for C₁₈H₁₃O₄NNa, 330.0737; found, 330.0785.

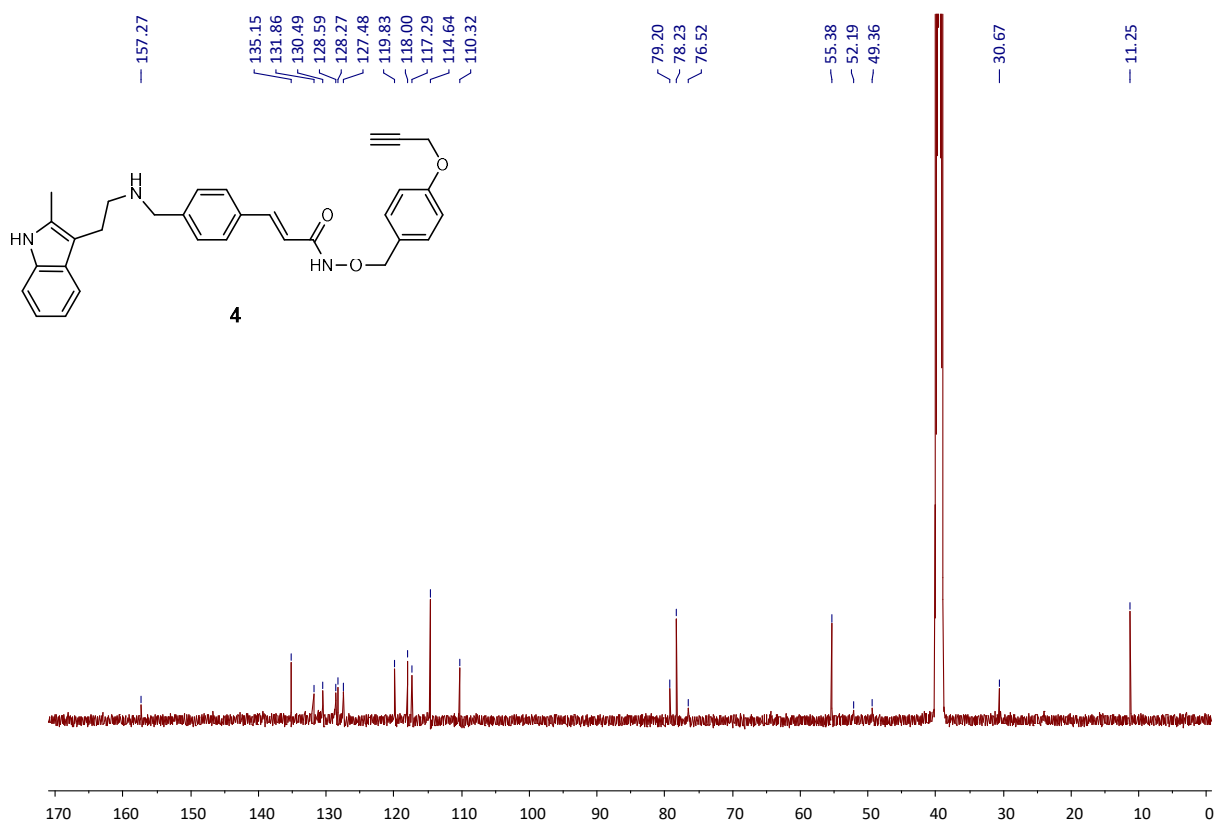
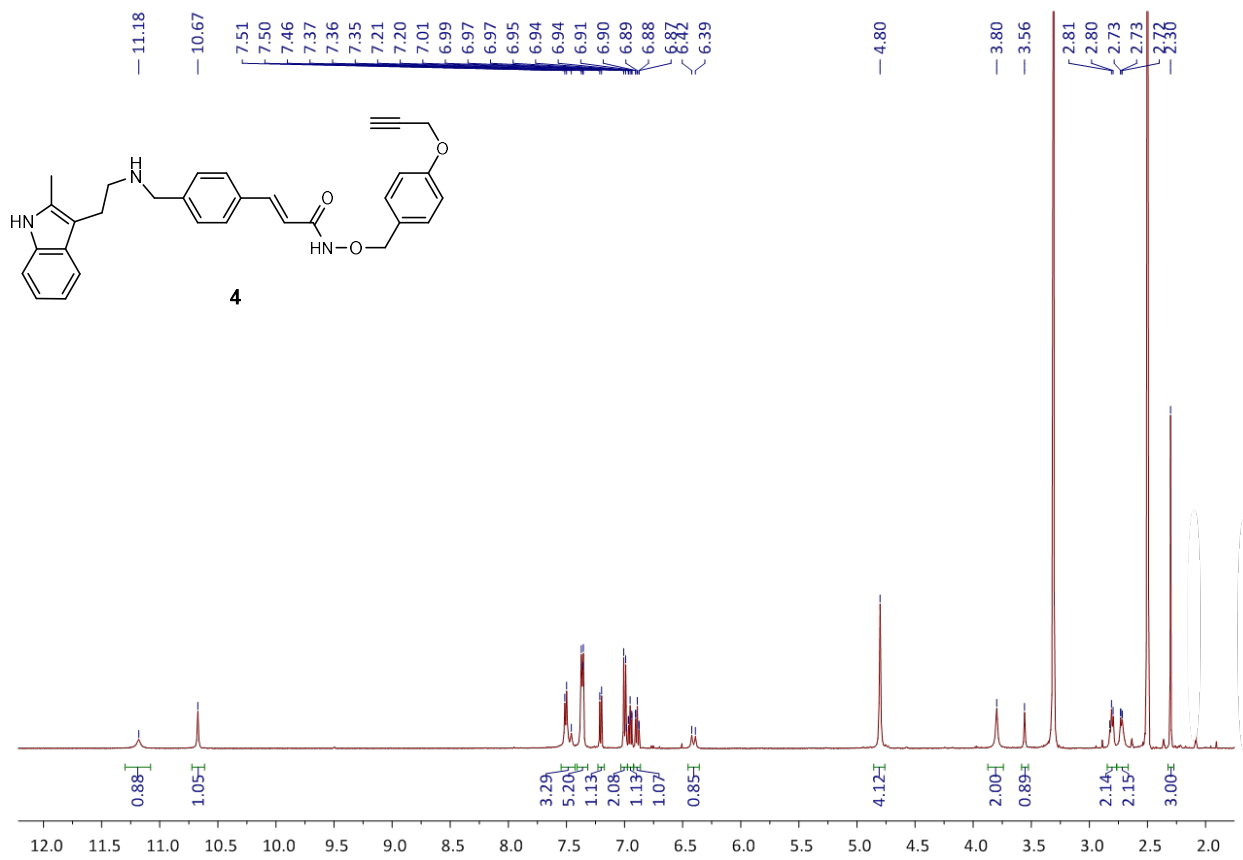
Synthesis of *O*-[4-(propargyloxy)benzyl]hydroxylamine HCl (7). Compound 6 (350 mg, 1.1 mmol) was dissolved in diethyl ether (6 mL) and treated with hydrazine monohydrate (2.2 mmol). The reaction mixture was stirred for 2 h at rt. Then, the solid residue was removed by filtration and HCl in ether (2 M, 4 mL) added to the filtrate with continuous stirring. The reaction was stirred for an additional 2 h and the resulting solid was filtered and dried yielding 7 as a white solid (190 mg, 78 % yield). **¹H NMR** (500 MHz, DMSO) δ 10.94 (s, 3H), 7.37 (d, *J* = 8.7 Hz, 2H), 7.03 (d, *J* = 8.7 Hz, 2H), 4.95 (s, 2H), 4.82 (d, *J* = 2.4 Hz, 2H), 3.58 (t, *J* = 2.4 Hz, 1H). **¹³C NMR** (126 MHz, DMSO) δ

157.83, 131.05 (CH x 2), 126.29, 114.92 (CH x 2), 79.06, 78.36 (CH), 75.39 (CH₂), 55.43 (CH₂). **HRMS** (m/z): [M]⁺ calcd for C₁₀H₁₂O₂N, 178.0863; found, 178.0885.

(*E*)-methyl 3-(4-{{2-(2-methyl-1*H*-indol-3-yl)ethylamino}methyl}phenyl)acrylate was synthesized according to literature.³

Synthesis of (*E*)-3-(4-{{2-(2-methyl-1*H*-indol-3-yl)ethylamino}methyl}phenyl)acrylic acid (9). To a solution of (*E*)-methyl 3-(4-{{2-(2-methyl-1*H*-indol-3-yl)ethylamino}methyl}phenyl)acrylate (140 mg, 0.40 mmol) in THF/ H₂O (1:5; 2.5 mL) was added dropwise an aqueous solution of NaOH 1N (0.5 mL). The resulting mixture was stirred at rt overnight and then acidified using aqueous solution of HCl 3N. The resulting precipitate was filtered, thoroughly washed with CH₃CN, and dried *in vacuo* to give rise an off-white solid (94 mg, 70 %). **¹H NMR** (500 MHz, DMSO) δ 10.65 (s, 1H), 7.58 (d, *J* = 8.1 Hz, 2H), 7.51 (d, *J* = 16.0 Hz, 1H), 7.35 (dd, *J* = 7.5, 5.4 Hz, 3H), 7.20 (d, *J* = 7.9 Hz, 1H), 6.94 (td, *J* = 7.5, 1.0 Hz, 1H), 6.88 (td, *J* = 7.5, 1.0 Hz, 1H), 6.46 (d, *J* = 16.0 Hz, 1H), 3.75 (s, 2H), 2.79 (t, *J* = 7.4 Hz, 2H), 2.67 (t, *J* = 7.3 Hz, 2H), 2.30 (s, 3H). **LC-MS** (m/z): 335.1544.

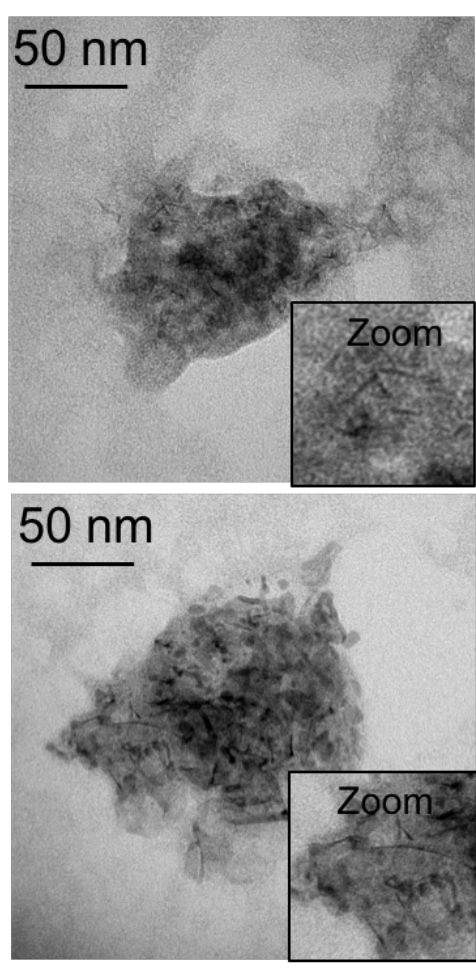
Synthesis of prodrug 4. Compound **9** (25 mg, 0.075 mmol) and **7** (24 mg, 0.112 mmol) were added to a 25 mL round-bottom flask and partially dissolved in distilled water (1 mL). *N*-(3-Dimethylaminopropyl)-*N'*-ethylcarbodiimide hydrochloride (43 mg, 0.225 mmol) was then added to the mixture. The pH was monitored and adjusted to 4.5 with a NaOH and / or HCl aqueous solution (1 M). The reaction was stirred for 6 h at rt and constant pH (4.5). Water was removed under reduced pressure, and crude suspended in acetonitrile and vacuum filtered. Solution was purified by semi-preparative TLC eluting with DCM:MeOH 7:3 giving rise a yellow solid (9.3 mg, 25%). **¹H NMR** (500 MHz, DMSO) δ 11.18 (bs, 1H), 10.67 (s, 1H), 7.49 (m, 3H), 7.36 (m, 5H), 7.21 (d, *J* = 7.9 Hz, 1H), 7.00 (d, *J* = 8.7 Hz, 2H), 6.95 (ddd, *J* = 8.1, 7.1, 1.2 Hz, 1H), 6.89 (ddd, *J* = 8.0, 7.1, 1.1 Hz, 1H), 6.41 (d, *J* = 15.8 Hz, 1H), 4.80 (s, 4H), 3.80 (s, 2H), 3.56 (s, 1H), 2.81 (m, 2H), 2.72 (m, 2H), 2.30 (s, 3H). **¹³C NMR** (126 MHz, DMSO) δ 157.27, 135.15, 131.86, 130.49, 128.59, 128.27, 127.48, 119.83, 118.00, 117.29, 114.64, 110.32, 79.20, 78.23, 76.52, 55.38, 52.19, 49.36, 30.67, 11.25. **HRMS** (m/z): [M]⁺ calcd. for C₃₁H₃₂O₃N₃, 494.2438; found, 494.2433. HPLC purity: > 95%; Rt: 5.52 min.



1.3. Physical and functional characterization

1.3.1. Electron microscopy: TEM imaging

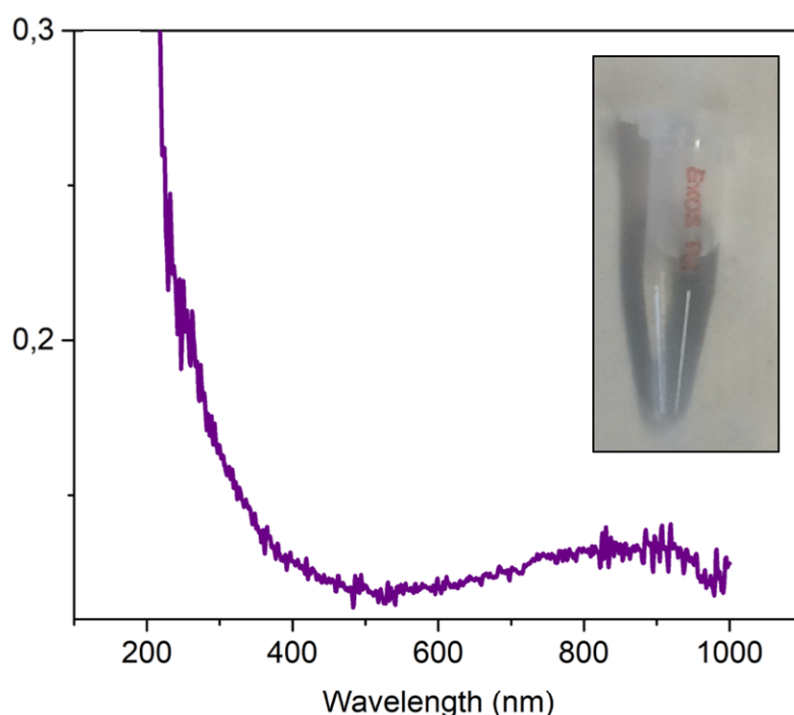
Transmission electron microscopy (TEM) observations were carried using a T20-FEI microscope with a LaB6 electron source fitted with a “SuperTwin®” objective lens allowing a point-to-point resolution of 2.4 Å. 5µL suspension of stained **Pd-Exo^{A549}** was pipetted onto a TEM copper grid with a holey carbon film. 10µL Phosphotungstic acid (3 %, contrast agent) solution was drop on the grid to stain the vesicles. Samples were let evaporate completely and then analyzed. Suppl. Fig. 2 shows TEM images of **Pd-Exo^{A549}** showing the Pd nanosheets generated within them without modifying their morphology and structure.



Suppl. Fig. 2. TEM images of **Pd-Exo^{A549}** stained with Phosphotungstic acid.

1.3.2. UV-VIS Spectroscopy

Optical properties of **Pd-Exo^{A549}** were studied using a UV-VIS spectroscopy (Jasco V670). As shown in Suppl. Fig. 3, a surface plasmon resonance peak was observed in the near infrared range, which corresponds to the expected absorbance peak of ultra-thin Pd nanosheets. This result is in agreement with the literature.⁴



Suppl. Fig. 3. *UV-VIS absorption spectrum of Pd-Exo^{A549} showing a maximum surface plasmon resonance peak at approx. 900 nm.*

1.3.3. Inductively coupled plasma mass spectrometry (ICP-MS)

The content of Pd loaded inside **Pd-Exo^{A549}** was quantified by inductively coupled plasma mass spectrometry (ICP-MS) and normalized by total protein amount in the exosomes. The **Pd-Exo^{A549}** total protein was determined by BCA assay as described in the manuscript. Normalized ICP-MS results demonstrated a relatively high amount of palladium inside the vesicles, with a value of 0.64 μg of Pd / μg of protein. The instrument for ICP-MS measurements (Elan DRC-e, PekinElmer, Germany), was equipped with a cross flow nebulizer and a Scott Double Pass spray chamber. Indium was employed as the internal standard for the elimination of the fluctuations coming from the sample preparation procedure and from the measuring conditions. The table below summarizes the main operational parameters. Exosome samples were diluted in 1 % Nitric Acid, 69.0-70% BAKER INSTRA-ANALYZED (Fisher Scientific, UK) and digested with 10 % Aqua regia. Calibrations were performed employing Pd standards with excellent correlations for all isotopes ($R=0.9994$ or higher). Samples were measured in triplicate. For the spike recovery test, 1.0791 ng mL^{-1} of a high concentrated Pd solution were added.

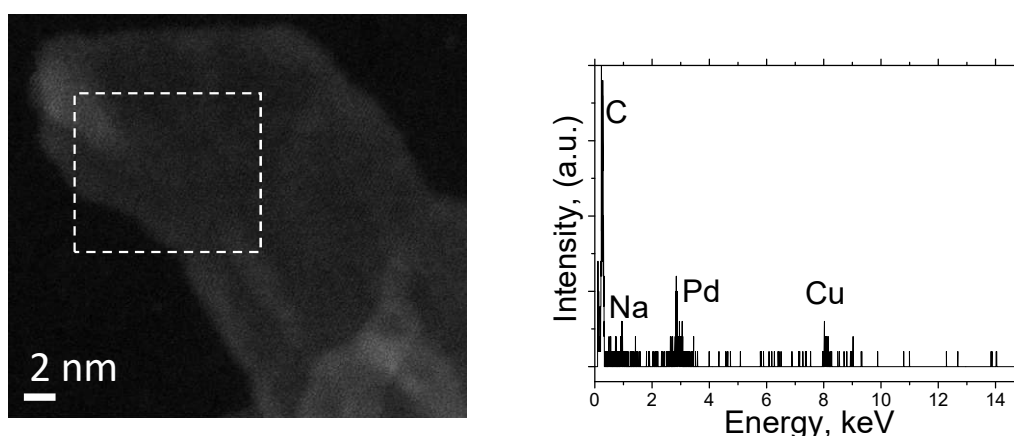
Nebulizer Gas Flow	0.93 l min ⁻¹
Auxiliary Gas Flow	1.2 l min ⁻¹
Plasma Gas Flow	15.00 l min ⁻¹
ICP RF Power	1200 W
Lens voltage	5.65 V
Analog Stage Voltage	-1900 V
Pulse Stage Voltage	1350 V
Detector	Dual
Detector mode	Pulse mode
Isotopes monitored	¹⁰² Pd, ¹⁰⁴ Pd, ¹⁰⁵ Pd, ¹⁰⁶ Pd, ¹⁰⁸ Pd, ¹¹⁰ Pd

The standard deviations of the Pd analysis by ICP-MS (i.e. on repeated measurements of the same sample) were less than 4% of the measured value. The standard deviation in the determination of the Pd/protein ratio (which includes the error of sampling and determination of Pd and total protein in independent samples) was 21.6%, i.e. the Pd content of the **Pd-Exo^{A549}** exosomes 0.64±0.138 µg of Pd / µg of protein.

Finally, a spike test was carried out adding a solution with a concentration of 1.0791 ng/mL. An average recovery of 86.7% was found for the different Pd isotopes.

1.3.4. Energy-dispersive X-ray spectroscopy analysis

Aberration corrected scanning transmission electron microscopy (Cs-corrected STEM-HAADF) images were acquired using a high angle annular dark field detector in a FEI XFEG TITAN electron microscope operated at 300 kV equipped with a CETCOR Cs-probe corrector from CEOS Company allowing formation of an electron probe of 0.08 nm. Elemental analysis was carried out with an EDS (EDAX) detector which allows performing EDS experiments in the scanning mode.

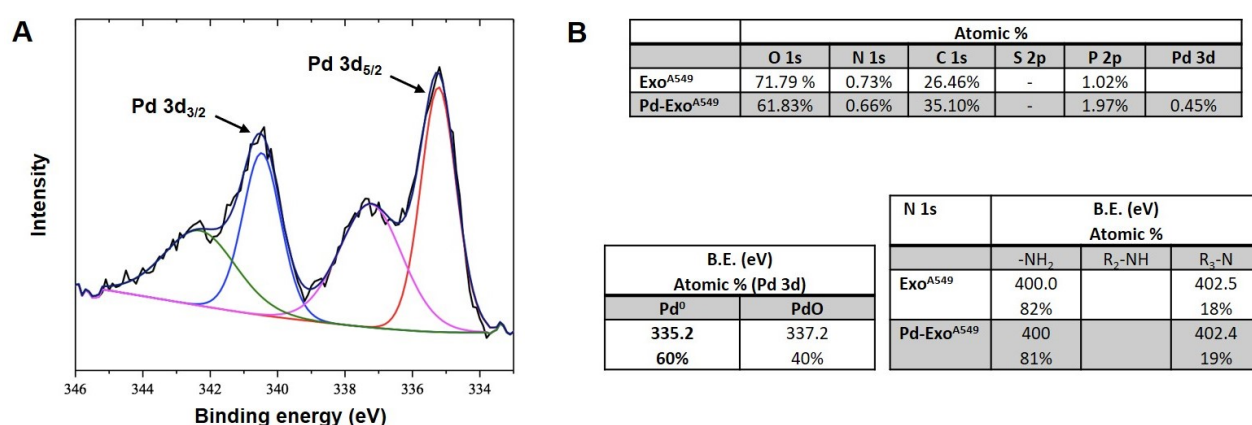


Suppl. Fig. 4. Energy-dispersive X-ray spectroscopy analysis (EDS) of **Pd-Exo^{A549}**. EDS analysis was carried out in the marked area of the STEM-HAADF image.

1.3.5. X-Ray Photoelectron Spectroscopy

The elemental composition of the **Pd-Exo^{A549}** and the chemical environment of Pd atoms were evaluated using X-Ray photoelectron spectroscopy (XPS) by using an Axis Supra (Kratos Analytical, UK). A monochromatic Al K α X-ray radiation ($h\nu= 1486.6$ eV) was employed as excitation source at 15 kV and 15 mA. The **Pd-Exo^{A549}** were previously deposited onto a cover slip and left to dry completely. The peaks analysis was carried out by the CasaXPS software (Casa Software Ltd, UK).

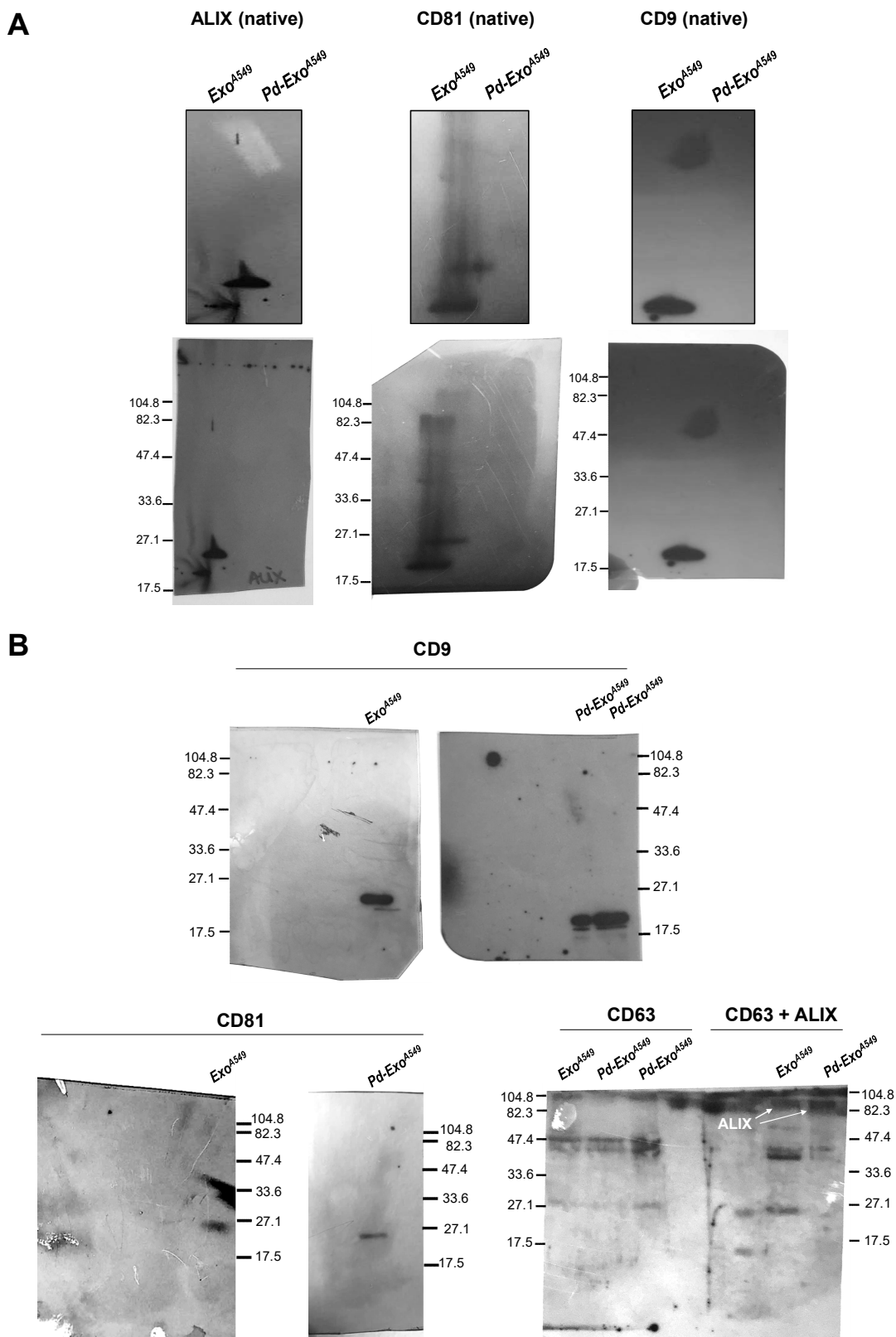
The core level Pd 3d_{3/2} centered at 335.2 eV was attributed to the presence of Pd⁰ in agreement with the previous literature.⁵



Suppl. Fig 5. (A) X-Ray Photoelectron Spectroscopy (XPS) spectrum of **Pd-Exo^{A549}**. **(B)** XPS analysis of **Exo^{A549}** and **Pd-Exo^{A549}**. The top table indicates the atomic composition percentage of **Exo^{A549}** and **Pd-Exo^{A549}**. The bottom left and right tables show the oxidation state of Pd 3d atoms of **Pd-Exo^{A549}** and N 1s atoms of **Exo^{A549}** and **Pd-Exo^{A549}**, respectively.

1.3.6. Native Western blot

Native Western Blot was performed against ALIX; 1:1000 (Cell Signaling Technologies, United States), CD9; 1:2000 (Abcam, UK) and CD81; 1:500 (Santa Cruz Biotechnology, United States) using 8 % acrylamide/bisacrilamide gels without SDS. **Exo^{A549}** and **Pd-Exo^{A549}** were lysed and precipitated with acetone, as previously mentioned. Samples were directly loaded onto the gels with a loading buffer composed by 62.5 mM Tris-HCl pH=6.8, 25 % glycerol and 0.01% bromophenol blue. Then, the electrophoresis was performed during 2 h at 100 v constant and the transference to the nitrocellulose membrane was carried out at 4 °C during 12 h at 300 mV constant. After the blocking step, the blotting was carried out incubating ALIX, CD9 and CD81 antibodies as described before.

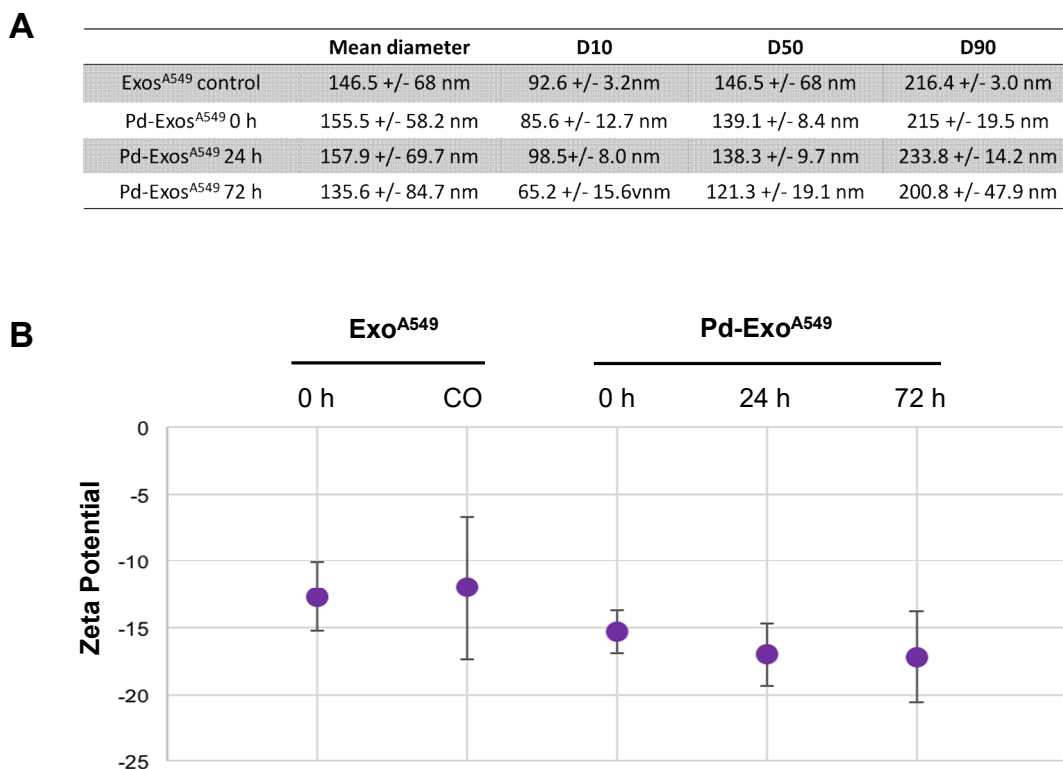


Suppl. Fig. 6. (A) Western blots of exosome-specific biomarkers ALIX, CD9 and CD81 of Exo^{A549} and Pd-Exo^{A549} under native (non-denaturing) conditions. Full blots with weight scales are shown below. **(B)** Full western blots with weight scales from which the bands of Figure 1f were taken.

1.3.7. Stability study

In order to evaluate the stability of the Pd-loaded exosomes, the particle size of Exo^{A549} and Pd-Exo^{A549} were analyzed at different time points using a Nanosight NS50 (Mavorn Instruments Ltd, Malvern, UK). Moreover, the zeta potential of Exo^{A549}, CO treated Exo^{A549} and Pd-Exo^{A549} was also measured by dynamic light scattering (DLS) at pH=7

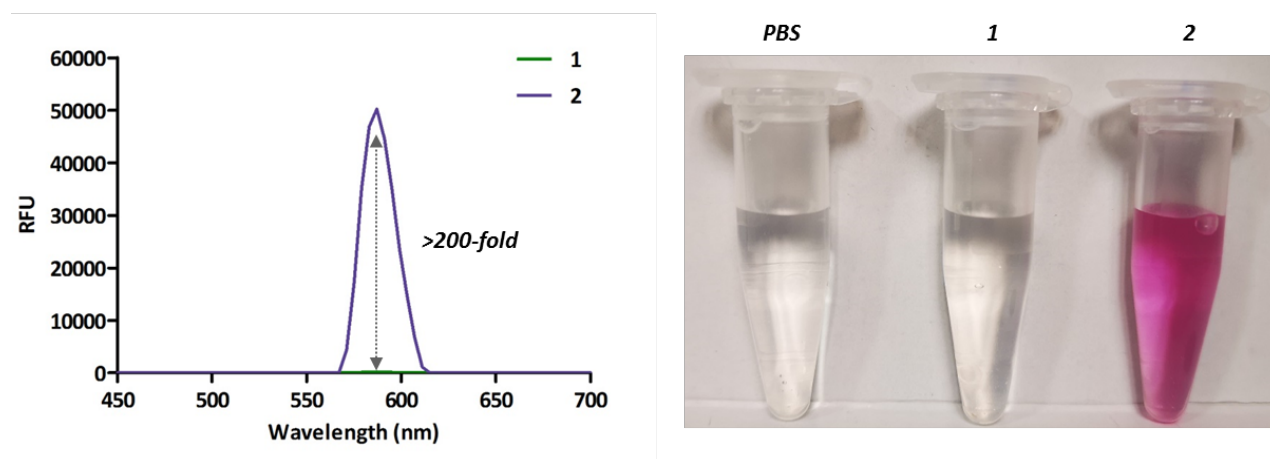
in a Brookhaven 90 Plus equipment using the ZetaPals software. Both the particle size and the zeta potential were evaluated at 3 time points (0, 24 and 72 h) after synthesis.



Suppl. Fig. 7. Stability study. (A) Particle size analysis of Exo^{A549} (t= 0h) and Pd-Exo^{A549} (t= 0, 24 and 72 h). Error bars: \pm SD, n = 3. (B) Zeta potential analysis of Exo^{A549} (before and after treatment with CO) and Pd-Exo^{A549} (t= 0, 24 and 72 h). Error bars: \pm SD, n = 2.

1.3.8. Fluorescence spectra of compounds 1 and 2

Solutions of compound **1** and **2** (25 μ M, pH 7.4) in PBS were prepared. The mixtures were shaken at 1200 rpm and 37°C in a Thermomixer for 10 min. Fluorescence was measured in a NanoDrop 3300 Fluorospectrometer (White LED excitation: 460-650 nm). PBS only was used as a blank.



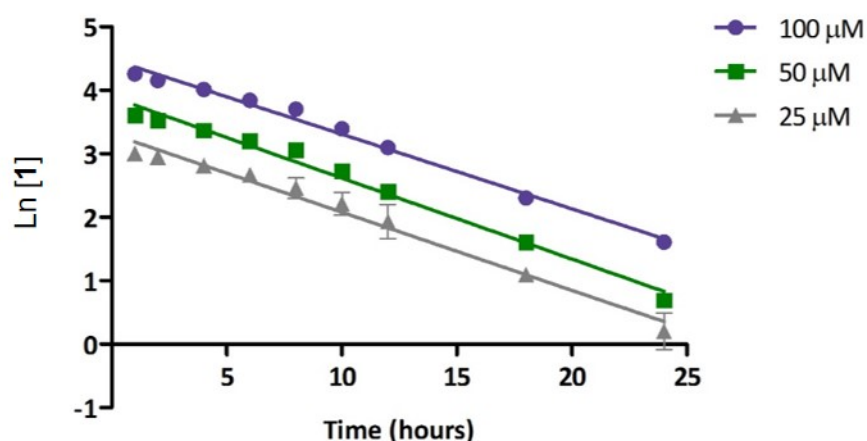
Suppl. Fig. 8. Left: Fluorescence spectra of sensor 1 and resorufin 2 (25 μ M) in PBS. Right: Eppendorf vials of blank solution (PBS), 1 and 2 (25 μ M) in PBS.

1.3.9. Time lapse imaging

Time-lapse microscopy and atomic emission spectroscopy allowed us to demonstrate and to visualize in real time the activation of **1** into **2** mediated by **Pd-Exo^{A549}**. We employed with a 20x objective (Ex/Em: 560/630 nm, Leica AF6000 LX, Germany) and non-fluorescent **1** alone as negative control and **2** alone as positive control. 1 μg of **Pd-Exo^{A549}** were added to a 20 μM solution of **1** in PBS (0.5 mL) in a 24-well plate and incubated for 24 h. Frames were taken every 15 min for 24 h in DIC mode and under red fluorescence emission. Movies were created using ImageJ software. As we can see in the frames presented in the videos of the supplementary material, when non-fluorescent **1** was observed in the presence of **Pd-Exo^{A549}** red fluorescence appears while time increases, thus indicating the catalytic conversion of **1** to **2**. After 24 h, the fluorescence levels were comparable with positive control conditions (**2** directly observed under time-lapse microscopy).

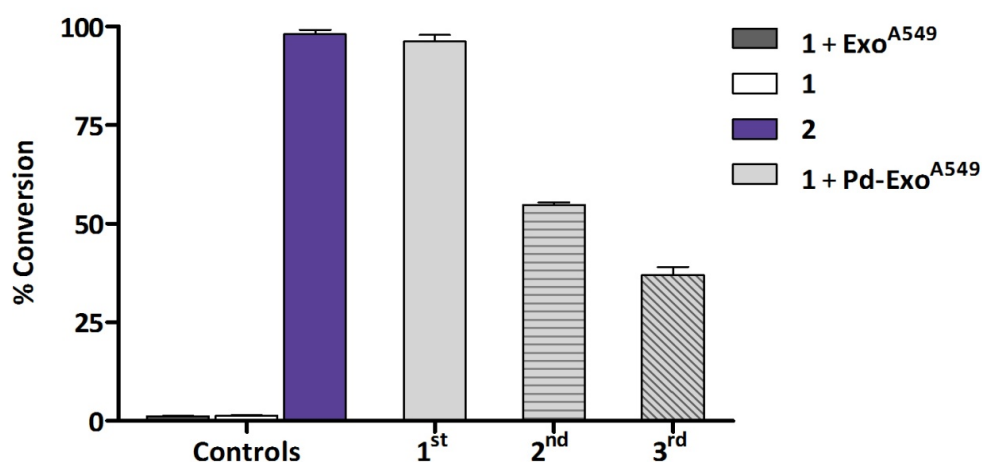
1.3.10. Determination of the reaction rate constant (K)

Pd-Exo^{A549} (1 μg of exosomes) were added to a 500 μL solution of reagent **1** (25, 50 and 100 μM) in PBS, to obtain a final concentration of 0.20 μg of **Pd-Exo^{A549}**/100 μL , respectively. The mixtures were shaken at 700 rpm and 37°C in a Thermomixer, and reactions were monitored overtime (1 h, 2-12 h every 2 hours, 18 h and 24 h) by fluorescence in a PerkinElmer EnVision 2101 multilabel reader (Ex/Em: 540 nm/590 nm). Samples were repeated in triplicate. Concentrations of product **2** (μM) were calculated based on the fluorescence signal of positive control resorufin at 25, 50 and 100 μM , and concentrations of substrate **1** were subtracted from the resulting product **2** (μM). The reaction rate constant K was estimated by a linear regression of the line plots of $\text{Ln}[1]$ overtime, providing K value equal to slope of the lines.



Suppl. Fig. 9. Kinetic study of the reaction of **Pd-Exo^{A549}** (0.2 μg /100 μL) with different concentrations of **1** (25, 50 and 100 μM) in PBS at 37 °C. Natural logarithmic values of the concentration of substrate **1** versus time. Curves fit: linear regression, $r^2 > 0.95$. Error bars: $\pm\text{SD}$, $n = 3$.

1.3.11. Recyclability study of Pd-Exo^{A549}



Suppl. Fig. 10. Recyclability assay of Pd-Exo^{A549} to mediate the O-depropargylation of sensor 1 (100 μ M) into fluorescent compound 2 during three catalytic cycles at 0.20 μ g of Pd-Exo^{A549}/100 μ L. Error bars: \pm SEM, $n = 3$.

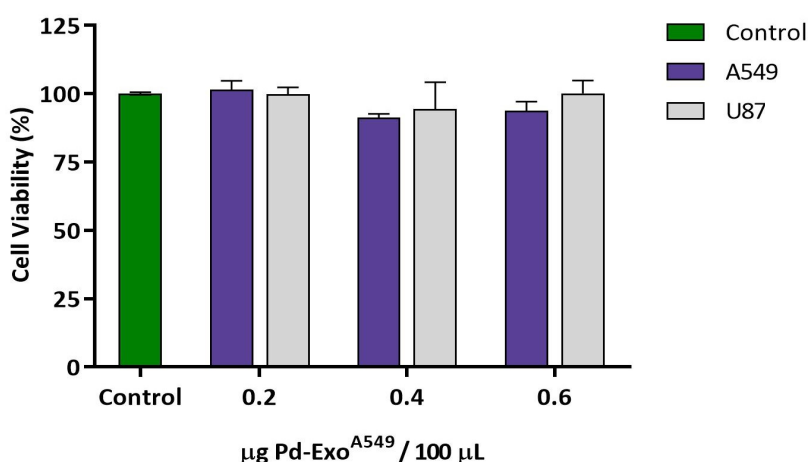
1.4. Biological experiments

Lung adenocarcinoma A549 cells, glioma U87 cells (gift from Dr Wilkinson and Dr Gammoh, respectively) and murine macrophage-like RAW 264.7 cells (gift from Prof Carragher; ATCC, TIB-71) were cultured in DMEM supplemented with 10 % of FBS and L-glutamine (2 mM). None of these cell lines are included in the register of misidentified cell lines (source: ICLAC database v9, updated on October 2018). Each cell line was checked for mycoplasma before use and maintained in normoxic conditions at 37 °C and 5% CO₂. For those experiments involving Exo^{A549}, Pd-Exo^{A549} and Pd-Exo^{U87}, DMEM was supplemented with exosome-depleted FBS (Gibco™) and L-glutamine (2 mM). For those studies included in sections 4.1, 4.3 - 4.8, cells were seeded in a 96-well plate at 1,500 cells / well for A549 and RAW 264.7, and 2,000 cells / well for U87 and incubated for 24 h before treatment.

1.4.1. Study of Pd-Exo^{A549} biocompatibility

A549 and U87 cells were plated as indicated in above. Each well was then replaced with a suspension of Pd-Exo^{A549} in culture media depleted of exosomes at 0.2, 0.4 and 0.6 μ g per 100 μ L for A549 cells or 0.26, 0.53 y 0.8 μ g per 100 μ L for U87 cells, and incubated for 6 h. Cells were then washed with PBS buffer and fresh media added. After 5 d, PrestoBlue™ cell viability reagent (10 % v/v) was added to each well and the plate incubated for 90 min. Fluorescence emission was detected using a PerkinElmer

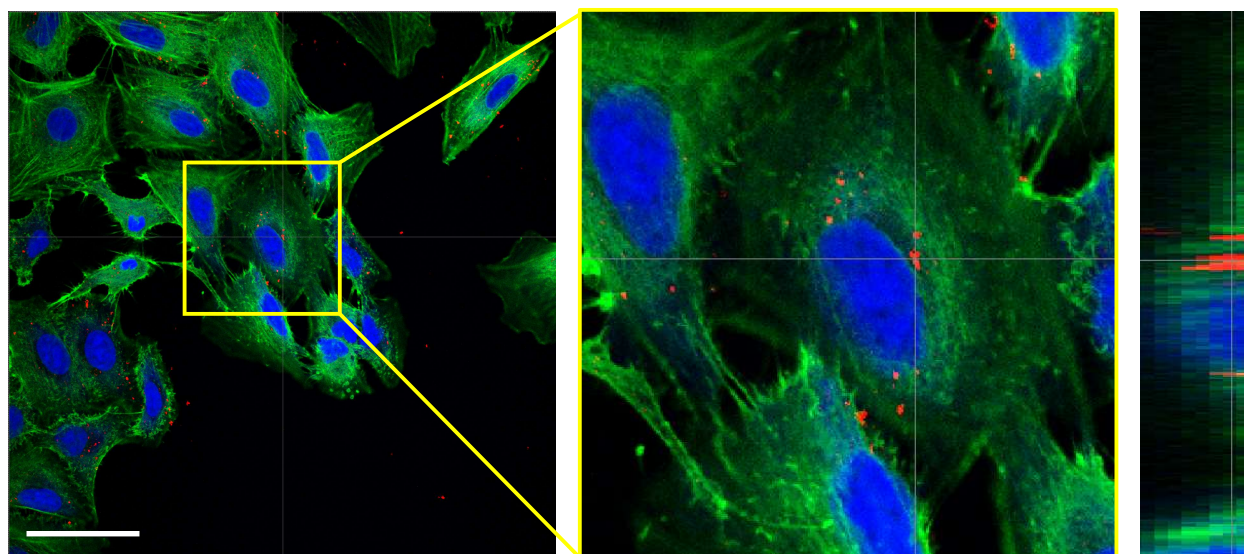
EnVision 2101 multilabel reader (Ex / Em: 540 / 590 nm). Experiments were performed in triplicates.



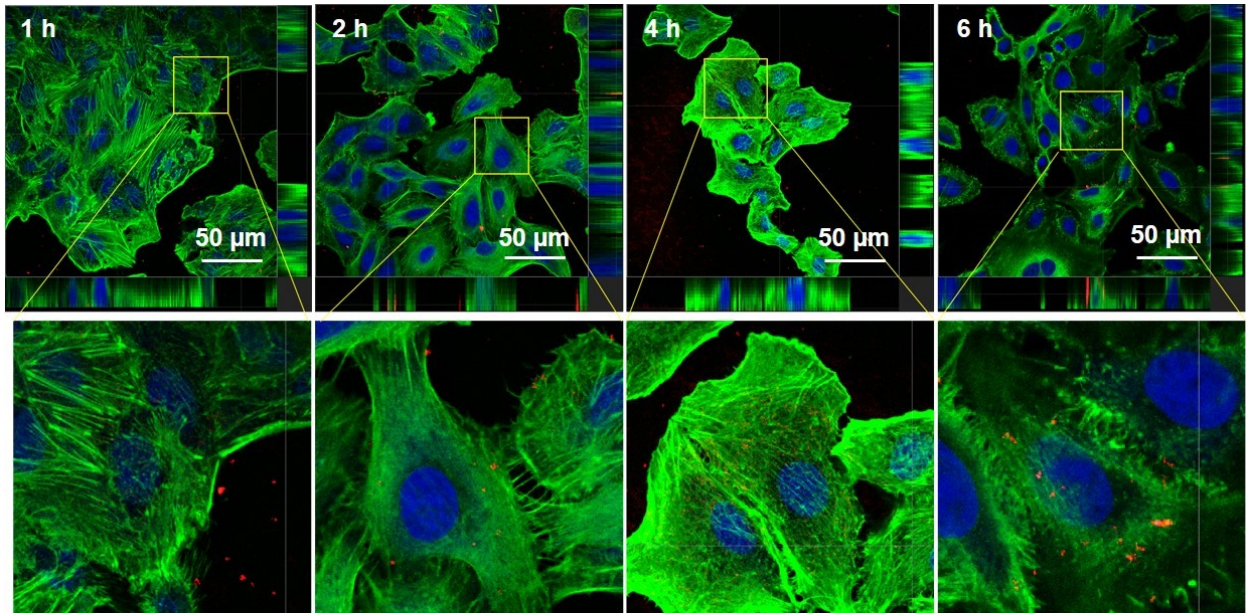
Suppl. Fig. 11. A549 and U87 cell viability study after treatment with **Pd-Exo^{A549}**. Cell viability was measured at day 5 using PrestoBlue[®] reagent. Error bars: \pm SEM, $n = 3$.

1.4.2. Confocal study of Pd-Exo^{A549} cell internalization

A549 cells were seeded at a density of 1.5×10^4 onto 20 mm cover slips (in a 24-well plate) and incubated under standard culture conditions for 24 h. 1 μ g of **Pd-Exo^{A549}** was then added to each well and incubated for additional 24 h. Cells were fixed with 4 % paraformaldehyde and stained with phalloidin-Alexa488 (Invitrogen) and Draq-5. Cells were imaged by confocal microscopy (Spectral Confocal Microscope Leica TCA SP2) with a 63x oil immersed N.A. 1.40 objective. Reflection of the incident light at 488/490 was used to directly visualize **Pd-Exo^{A549}**. Z-stack orthogonal projections were used to visualize the presence of exosomes inside cells cytosol.

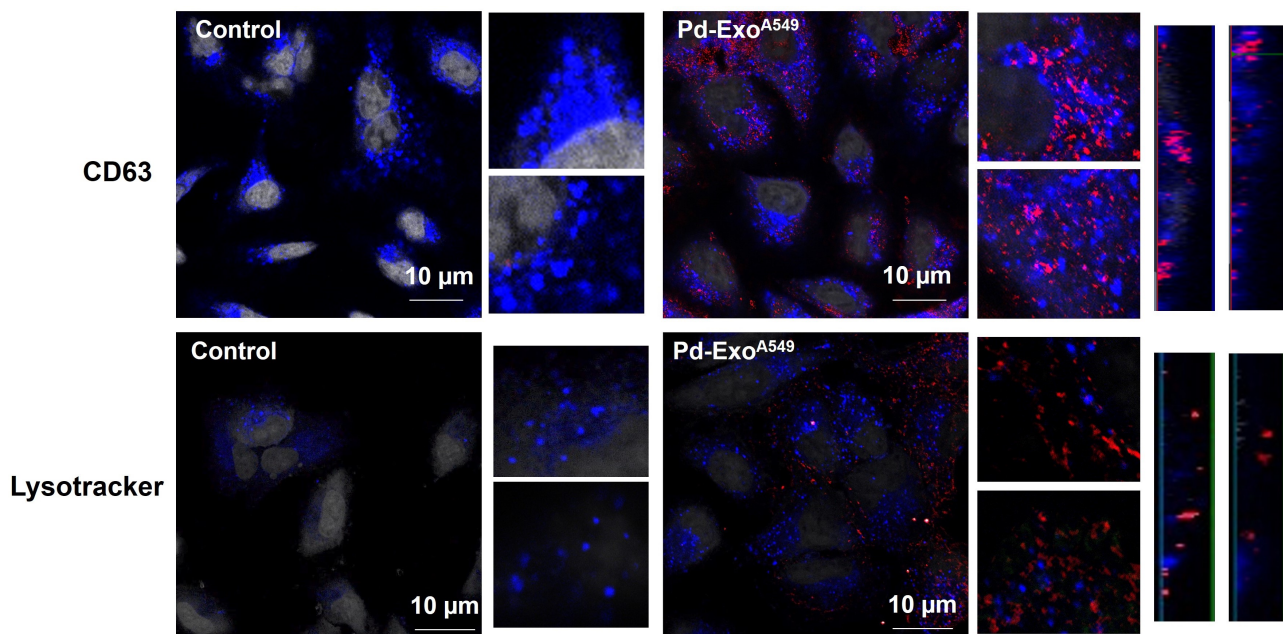


Suppl. Fig. 12. Merged confocal images of A549 cells after treatment with **Pd-Exo^{A549}** for 24 h. Actin fibers (phalloidin-488) are shown in green, cell nuclei (Draq5) in blue and clusters of **Pd-Exo^{A549}** in red. Scale bar= 50 μ m. The middle and left image show the amplified and z-stacks sections, respectively.



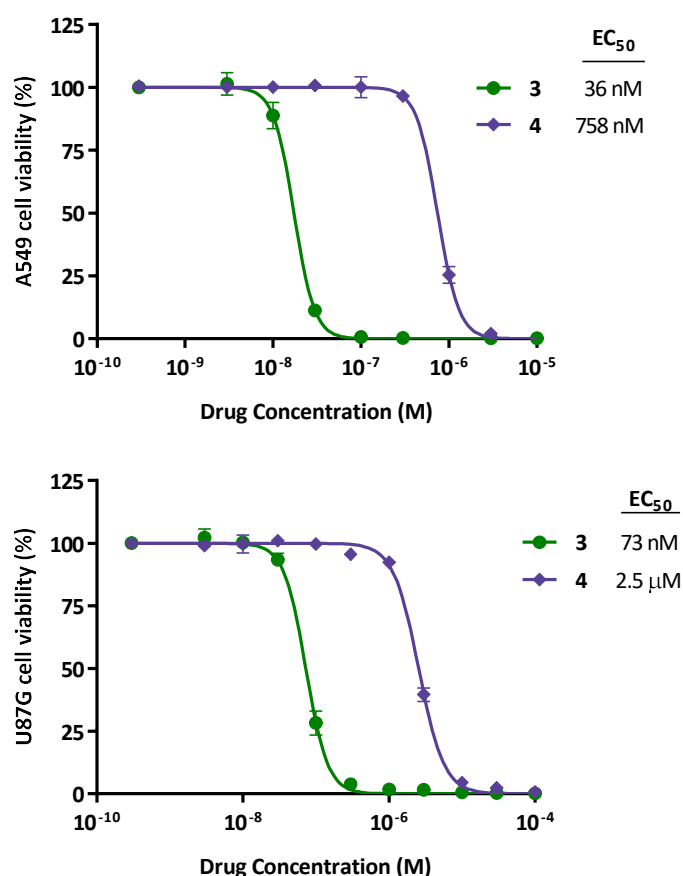
Suppl. Fig. 13. Merged confocal images of A549 cells after treatment with **Pd-Exo^{A549}** for 1 h, 2 h, 4 h and 6 h. Actin fibers (phalloidin-488) are shown in green, cell nuclei (Draq5) in blue and clusters of **Pd-Exo^{A549}** in red. Scale bar= 50 μm. Lower panel: Quantitative analysis of red fluorescent intensity in the cells at different timepoints. Error bars: ±SD, n = 2.

We have also employed confocal microscopy to monitor the association of **Pd-Exo^{A549}** with the endo-lysosomal pathway (Spectral Confocal Microscope Leica TCA SP2 and ZEISS LSM880 Confocal Laser Scanning Microscope). To this end, A549 cells were seeded onto a cover slip and were incubated with **Pd-Exo^{A549}** for 6 h. Then, they were fixed with 4 % PFA as previously mentioned. Endosomes and exosomes were labeled with a specific CD63-Alexa-488 antibody (Thermo Fisher Scientific, USA), the nuclei were stained with Draq-5 (gray) and the **Pd-Exo^{A549}** were directly observed by reflection of the incident light in the microscope at 488/490 nm ex/em. For lysosomes labeling, cells were firstly marked with LysoTracker Green (Invitrogen, USA) following manufacturer instructions. Then, cells were fixed with 4 %PFA. Z-stack orthogonal projections from confocal laser-scanning microscopy study were employed to determine the presence of Pd within the endo-lysosomal pathway.



Suppl. Fig. 14. Confocal study of the intracellular location of **Pd-Exo^{A549}** after incubation for 6 h with A549 cells. After treatment, cells were fixed and labelled with Draq5 (grey) and either a specific CD63-Alexa488 antibody or lysotracker (blue). **Pd-Exo^{A549}** were directly observed by reflection of the incident light (red). The right images show the amplified and z-stacks sections. Control= untreated cells.

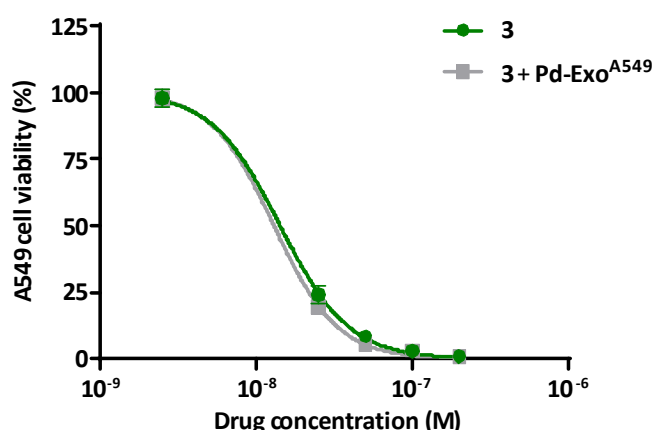
1.4.3. Cell viability study in A549 and U87 cells: 4 vs 3



Suppl. Fig. 15. Dose-response curves after 5 d treatment with **3** and **4** in A549 (top) and U87 cells (bottom). Curves fit: sigmoidal variable slope curves. Error bars: \pm SEM, $n = 3$.

1.4.4. Synergistic cytotoxic study between **3** and Pd-Exo^{A549} in A549 cells

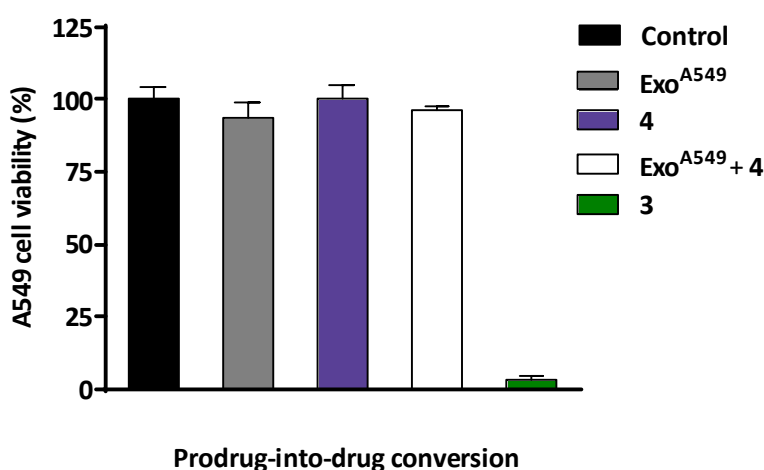
A549 cells were plated as indicated in above. The corresponding wells were then replaced with a suspension of **Pd-Exo^{A549}** in culture media depleted of exosomes at 0.4 μ g / 100 μ L and incubated for 6 hours. These wells were washed with PBS buffer to remove extracellular vesicles and treated with fresh media containing either DMSO (0.1% v/v) or **3** (0.025-0.2 μ M). Cells treated with **3** at 0.025-0.2 μ M were used as positive controls. After 5 d of treatment, cell viability was determined as described above. Experiments were performed in triplicates.



Suppl. Fig. 16. A549 dose-response curves after 5 d treatment with **3** (0.025-0.2 μ M) in the presence and absence of 0.4 μ g / 100 μ L of **Pd-Exo^{A549}**. Curves fit: sigmoidal variable slope curves. Error bars: \pm SEM, $n = 3$.

1.4.5. Exo^{A549} -mediated uncaging of **4** in A549 cells

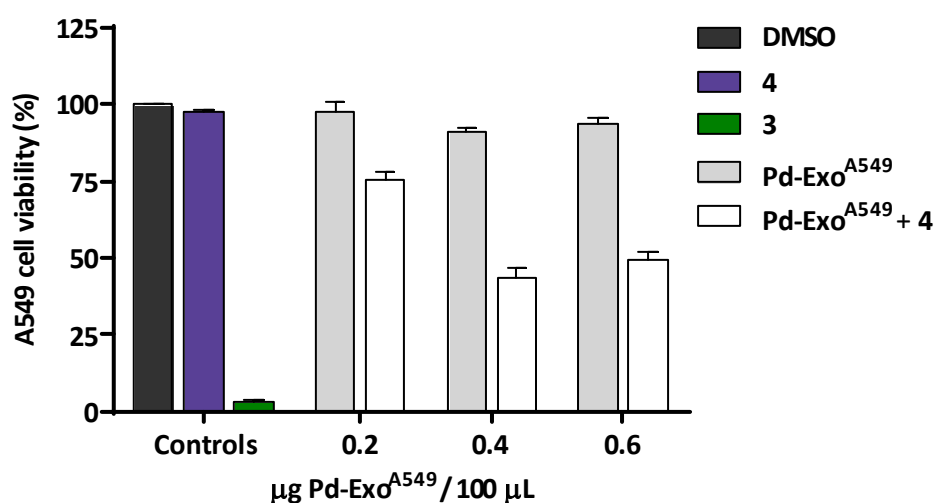
A549 cells were plated as indicated in above. The corresponding wells were then replaced with a suspension of Exo^{A549} in culture media depleted of exosomes at $0.4 \mu\text{g} / 100 \mu\text{L}$. After 6 h of incubation, these wells were washed with PBS buffer to remove extracellular vesicles and treated with fresh media containing either DMSO (0.1% v/v) or **4** ($0.2 \mu\text{M}$). Cells treated with **3** and **4** at $0.2 \mu\text{M}$ were used as positive and negative controls, respectively. After 5 d of treatment, cell viability was determined as described above. Experiments were performed in triplicates.



Suppl. Fig 17. Study of the potential Exo^{A549} -mediated uncaging of **4** inside cells. A549 cells were incubated for 6 h with $0.4 \mu\text{g} / 100 \mu\text{L}$ of Exo^{A549} . Cells were thoroughly washed to eliminate extracellular vesicles followed by addition of prodrug **4** ($0.2 \mu\text{M}$). Controls: Exo^{A549} only (–ve control, grey); prodrug **4** only (–ve control, purple); **3** (+ve control, green). Cell viability was measured at day 5 using PrestoBlue. Error bars: \pm SEM, $n = 3$.

1.4.6. Pd- Exo^{A549} -mediated activation of **4** at a range of concentrations

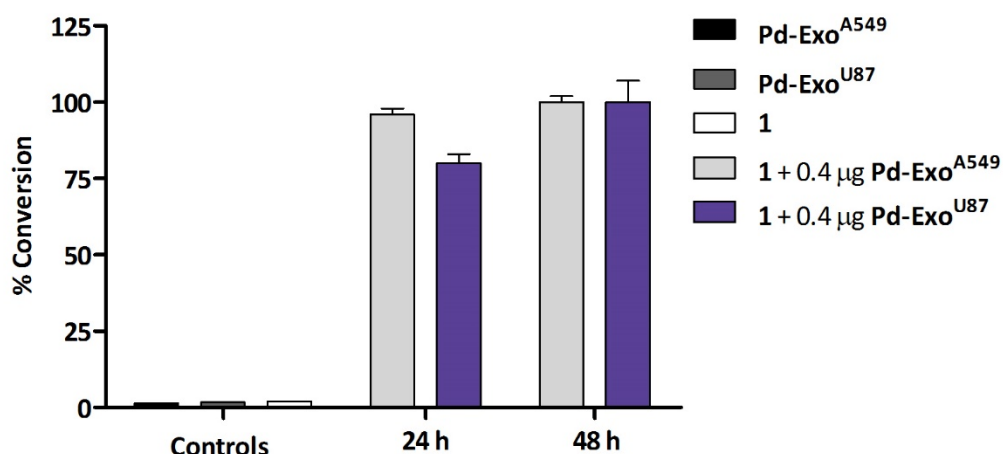
A549 cells were plated as indicated in above. The corresponding wells were then replaced with a suspension of Pd- Exo^{A549} in culture media depleted of exosomes at 0.2, 0.4 or $0.6 \mu\text{g} / 100 \mu\text{L}$. After 6 h of incubation, these wells were washed with PBS buffer to remove extracellular vesicles and treated with fresh media containing either DMSO (0.1% v/v) or **4** ($0.2 \mu\text{M}$). Cells treated with **3** and **4** at $0.2 \mu\text{M}$ were used as positive and negative controls, respectively. After 5 d of treatment, cell viability was determined as described above. Experiments were performed in triplicates.



Suppl. Fig. 18. *Pd-Exo^{A549}-mediated uncaging of 4 inside cells.* A549 cells were incubated for 6 h with 0.2, 0.4 and 0.6 µg / 100 µL. Cells were thoroughly washed to eliminate extracellular vesicles and prodrug **4** added (0.2 µM). Controls: **Pd-Exo^{A549}** only (–ve control, light grey); prodrug **4** only (–ve control, purple); **3** (+ve control, green). Cell viability was measured at day 5 using PrestoBlue. Error bars: ± SEM, n = 3.

1.4.7. Catalytic properties of Pd-Exo^{A549} versus Pd-Exo^{U87}

2 µg of **Pd-Exo^{A549}** or **Pd-Exo^{U87}** were added to a 500 µL solution of reagent **1** (100 µM) in PBS, to obtain a final concentration of 0.40 µg of **Pd-Exo^{A549}** or **Pd-Exo^{U87}**/100 µL, respectively. The mixtures were shaken at 700 rpm and 37 °C in a Thermomixer, and reactions were monitored after 24 and 48 h using a PerkinElmer EnVision 2101 multilabel reader (Ex/Em: 540 /590 nm). Sensor **1** alone (100 µM) or 0.40 µg of **Pd-Exo^{A549}** or **Pd-Exo^{U87}**/100 µL alone were used as negative controls and fluorescent dye **2** at 100 µM as reference control. Reactions were done in triplicates and the conversion % calculated according to the reference control.

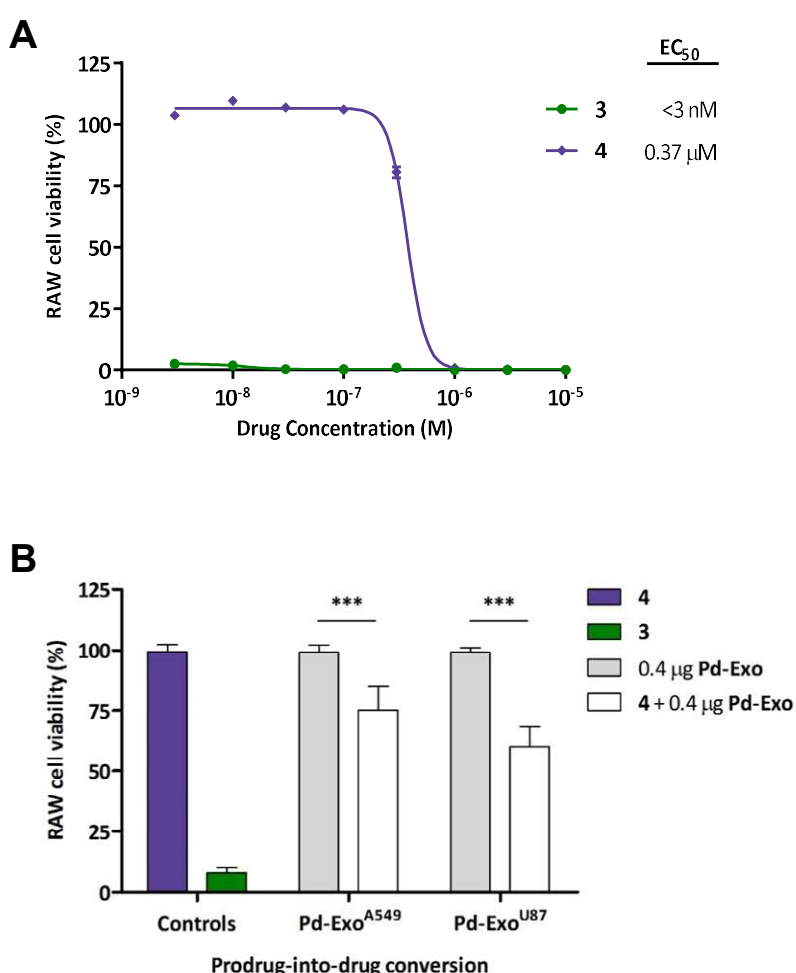


Suppl. Fig. 19. *Pd-Exo mediated conversion of non-fluorescent 1 into highly red-fluorescent resorufin 2 under biocompatible conditions (37 °C, PBS, pH 7.4, isotonicity).* Conversion efficiency after 24 h or 48 h incubation of **1** (100 µM) with **Pd-Exo^{A549}** or **Pd-Exo^{U87}** (0.4 µg / 100 µL). Conversion values (%) were calculated from fluorescence intensity measurements at $\lambda_{ex/em} = 540/590$ nm using the fluorescence intensity of **2** (100 µM) as 100 %. Negative controls: **1** (100 µM), **Pd-Exo^{A549}** or **Pd-Exo^{U87}** (0.4 µg / 100 µL). Error bars: ±SD, n=3.

1.4.8. Cell viability and intracellular prodrug activation study in RAW cells

RAW cells were plated as indicated in above. For cell viability assay, each well was then replaced with fresh media, containing compounds **3** and **4** (0.003-100 μM). Untreated cells were incubated with DMSO (0.1 % v/v).

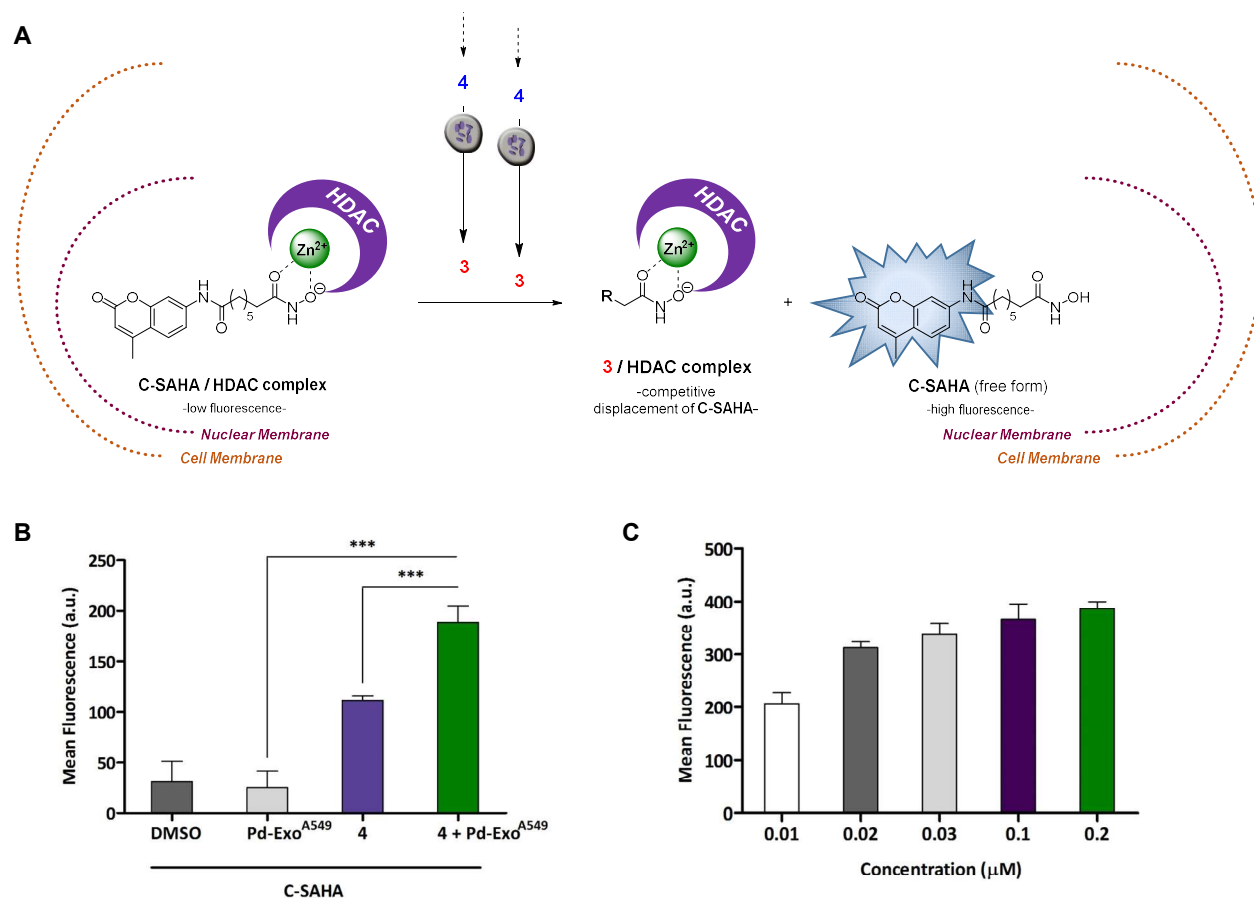
For intracellular prodrug activation assay, the corresponding wells were then replaced with a suspension of **Pd-Exo**^{A549} or **Pd-Exo**^{U87} in culture media depleted of exosomes (at 0.4 μg / 100 μL). After 6 h of incubation, these wells were washed with PBS buffer to remove extracellular vesicles and treated with fresh media containing either DMSO (0.1% v/v) or **4** (0.2 μM). Cells treated with **3** and **4** at 0.2 μM were used as positive and negative controls, respectively. After 5 d of incubation, cell viability was determined as described above. All conditions were normalized to the untreated cells (100 %) and curves fitted using GraphPad Prism using a sigmoidal variable slope curve. Experiments were performed in triplicates.



Suppl. Fig. 20. (A) RAW 264.7 dose-response curves after 5 d treatment with **3** and **4**. Curves fit: sigmoidal variable slope curves. Error bars: \pm SEM, $n = 3$. **(B)** Pd-Exo-mediated uncaging of **4** inside RAW 264.7 cells. Cells were incubated for 6 h with 0.4 μg / 100 μL of either Pd-Exo^{A549} or Pd-Exo^{U87}. Cells were thoroughly washed to eliminate extracellular vesicles followed by addition of prodrug **4** (0.2 μM). Controls: Pd-Exo^{A549} / Pd-Exo^{U87} only (–ve control, grey); prodrug **4** only (–ve control, purple); **3** (+ve control, green). Cell viability was measured at day 5 using PrestoBlue. Error bars: \pm SEM, $n = 3$. *** $P < 0.001$ (ANOVA).

1.4.9. Target engagement assay

A549 cells were seeded in a 96-well plate format (at 5,000 cells / well) and incubated for 24 h before treatment. The corresponding wells were then replaced with a suspension of **Pd-Exo**^{A549} in culture media depleted of exosomes (at 1.4 μg / 100 μL in order to normalize exosome quantity per number of seeded cell) containing coumarin-SAHA (C-SAHA) at 1 μM . After 6 h of incubation, these wells were washed with PBS buffer to remove extracellular vesicles and treated with fresh media containing either DMSO (0.1% v/v) or **4** (0.2 μM). Cells treated with **3** and **4** at 0.2 μM were used as positive and negative controls, respectively. Cells treated with **3** (0.2, 0.1, 0.03, 0.02 and 0.01 μM) were used for the standard curve. After 12 hours of incubation, cells were washed by centrifugation and analysed by flow cytometry (Ex / Em = 405 / 450 nm) using a BD LSRFortessa X-20. A one-way analysis of variance (ANOVA) was performed using Sigmastat 3.5 statistical analysis software. Experiments were performed in triplicates.



Suppl. Fig. 21. (A) Fluorescent study of the intracellular conversion of **4** into **3** by **Pd-Exo**^{A549}. Upon release of **3**, HDAC-bound fluorescently-quenched C-SAHA is competitively displaced from the catalytic site of the enzyme, resulting in a fluorescent signal ($\lambda_{ex/em}$ = 405/450 nm). **(B)** Mean fluorescence of A549 cells analyzed by flow cytometry after treatment with C-SAHA and: DMSO, only **Pd-Exo**^{A549}, only **4**, or **Pd-Exo**^{A549} (6h) followed by **4**. Experiments were incubated for 12 h. Error bars: \pm SD from $n = 3$; $p < 0.001$, *** (ANOVA). **(C)** Mean fluorescence of A549 cells analyzed by flow cytometry after treatment with C-SAHA (6 h) and **3** at different concentrations (0.01-0.2 μM).

2. SUPPLEMENTARY REFERENCES

- (1) Binauld, S.; Damiron, D.; Hamaide, T.; Pascault, J.-P.; Fleury, E.; et al. Click chemistry step growth polymerization of novel α -azide- ω -alkyne monomers. *Chem. Commun.* **35**, 4138-4140 (2008).
- (2) High, A.; Prior, T.; Bell, R. A.; Rangachari, P.K. Probing the "Active Site" of Diamine Oxidase: Structure-Activity Relations for Histamine Potentiation by O-Alkylhydroxylamines on Colonic Epithelium. *J. Pharmacol. Exp. Ther.* **288**, 490-501 (1999).
- (3) Wang, H.; Yu, N.; Chen, D.; Lee, K. C.; Lye, P. L.; et al. Discovery of (2*E*)-3-{2-Butyl-1-[2-(diethylamino)ethyl]-1*H*-benzimidazol-5-yl]-*N*-hydroxyacrylamide (SB939), an Orally Active Histone Deacetylase Inhibitor with a Superior Preclinical Profile. *J. Med. Chem.* **54**, 4694-4720 (2011).
- (4) Huang, X.; Tang, S.; Mu, X.; Dai, Y.; Chen, G.; et al. Freestanding palladium nanosheets with plasmonic and catalytic properties. *Nat. Nanotech.* **6**, 28-32 (2011).
- (5) Huang, F.; Jia, Z.; Diao, J.; Yuan, H.; Su, D.; et al. Palladium nanoclusters immobilized on defective nanodiamond-graphene core-shell supports for semihydrogenation of phenylacetylene, *J. Energy Chem.* **33**, 31-36 (2019).